*Int. J. Multiphase Flow* Vol. 7, pp. 115–127
Pergamon/Elsevier, 1981. Printed in Great Britain

0301-9322/81/0201-0115/$02.00/0

# SHOCK WAVE-INDUCED BUBBLE MOTION

S. P. KALRA and Y. ZVIRIN†

Nuclear Safety and Analysis Department, Electric Power Research Institute, Palo Alto, CA 94303, U.S.A.

(*Received* 28 *September* 1979; *in revised form* 1 *August* 1980)

**Abstract**—There is a lack of data on transient interphase shear forces on bubbles. The present work is an experimental and analytical investigation of unsteady bubble motions induced by shock waves. Bubble trajectories were monitored in a shock tube using high-speed Schlieren photographs. Pressure histories at two locations weere used to determine the average wave speed in the bubbly mixture. An equation of motion was developed and solved for predicting the bubble trajectories and velocities. Reasonable agreement is obtained between the experimental results and the analytical predictions. It was found that for experimental range of Reynolds numbers (200–12,000), a constant drag coefficient $c_D \simeq 2.6$ can be utilized to estimate the drag force.

## INTRODUCTION

The two-fluid formulation of transient two phase flows requires expressions for interphase shear. The available data on shear forces associated with transient bubble motions are quite scarce. Such data is important, for example, in understanding the flashing due to sudden decompression of a pressurized system, e.g. the primary coolant in Pressurized Water Reactors. (PWRs). Presently, there is a lack of data on unsteady bubble trajectories and velocity profiles. One method to obtain such data is to accelerate bubbles by the interaction with shock waves. Previous studies, however, looked at the structure of the waves, the behavior of the pressure, the shock velocity, the shock relations for void fractions, etc. but there is still a lack of information on the motion of the bubble after the shock.

Crespo (1969) investigated the effects of the relative motion of gas bubbles in liquid and their mass fraction fluctuations in the wave velocities. He also found that the shock structure depends on both low- and high-frequency Mach numbers: when both are larger than one, the pressure behind the shock oscillates. The oscillations disappear when the latter is smaller than one.

Van-Wijngaarden *et al.* (1968), (1970), (1972), Noordzij (1974) and Prosperetti (1976) concentrated efforts on the equation of motion and the shock structure in bubbly flows, especially on the unsteady pressure behavior. The experiments reported by Campbell & Pitcher (1958), Noordzij (1973), Nyer & Schrock (1967) and Gel'fand *et al.* (1975) generally dealt with measurements of wave speed and attenuation of pressure oscillations in the bubbly mixture. Cambell & Pitcher (1958) also developed isothermal jump conditions for pressures, velocities and void fractions. The results were extended by Noordzij & van Wijngaarden (1974) for adiabatic jump conditions.

The steady motion of bubbles in liquids has been studied quite extensively. Peebles & Garber (1953) summarized the results for drag coefficient on bubbles in various liquids and for a wide range of flow conditions, determined by the Reynolds number. They also discussed the bubble geometries and deformations. Ishii & Zuber (1979) developed drag coefficients and correlations for relative two phase dispersed motions. Their derivation is based on simplified similarity criteria and a mixture viscosity model. Moore (1965) investigated the terminal rise velocity of a bubble in a pure liquid and the effects of the bubble distortion on the drag coefficient for low Reynolds numbers.

For accelerating flows of solid particles, considerable changes of the drag coefficient, $c_D$, may take place. Lugt & Haussling (1978) studied numerically the start from rest of a thin cylindrical body in a viscous fluid. Their results show that $c_D$ increases by an order of

†On leave from: Faculty of Mechanical Engng, Technion, IIT, Haifa, Israel.

magnitude and then decreases to about the "regular" steady-state value during a short time. This phenomenon is caused by the starting vortices behind the leading and trailing edges. Another interesting phenomenon was discovered by Tyler & Salt (1978), namely, periodic oscillations of the drage force on solid spheres in accelerating flows (caused by a passage of a shock wave). This behavior is attributed, again, to the formation and abrupt detachment of low pressure vortices in the wake. They found an increase of 10–20 per cent above the steady-state value of the drag coefficient.

Karanfilian & Kotas (1978) experimentally studied the drag on a solid sphere subjected to a simple harmonic motion in a viscous liquid. They correlated the data by a correction factor for the drag coefficient, which depends on the ratio of the acceleration and the square of the velocity.

As mentioned above, information on drag coefficients for accelerating bubbles is still not available. Morrison & Stewart (1976) showed that the drag differs significantly than that for solid particles. They used Fourier transform to obtain relative magnitude and phase angles (as functions of the frequency of oscillations) for low Reynolds numbers.

This paper includes an analytical and experimental investigation of the unsteady bubble motion behind a shock wave. The motion is governed by wave-induced fluid flow, interfacial drag, buoyancy and bubble geometry. Therefore, the bubble trajectories are dominated by an unsteady relative motion between the two phases, induced by the shock wave. An equation for the bubble motion is derived, taking into account all these effects, where the history of the bubble distortion is included in the form of the Basset force (see Landau & Lifshitz 1959). The equation is solved for low and high Reynolds numbers to yield the bubble velocity.

The experiments consisted of shock wave propagations in bubbly mixtures of low void fractions. The propagation speed of the shock in the two-phase mixture was measured and the liquid velocity was derived from these measurements. High-speed Schlieren photography was used to trace bubble trajectories; the bubble velocities were determined from these measurements.

The analytical results are compared to the experimental data. It is shown that for the high Reynolds number range (2000–12,000), a constant drag coefficient $c_D = 2.6$ can be utilized to estimate the drag force. The effect of the Basset force in this range is negligible.

## ANALYSIS

The equation of motion of a bubble can be written in the following form† (see Brodkey 1967, van-Wijngaarden 1970 and Noordij & van-Wijngaarden 1974):

$$\frac{\mathrm{d}}{\mathrm{d}t}[\lambda\rho V w] = -V\frac{\mathrm{d}p}{\mathrm{d}x} - c_D A\frac{1}{2}\rho|w|w - (\rho-\rho_G)V_G - \frac{3}{2}\pi\rho D^2\left(\frac{\nu}{\pi}\right)^{1/2}\int_0^t \frac{\mathrm{d}w/\mathrm{d}t'}{\sqrt{(t-t')}}\mathrm{d}t' \qquad [1]$$

where the relative velocity $w$ is defined by

$$w = u - v, \qquad [2]$$

$u$ and $v$ are the liquid and bubble velocities, taken as positive in the downward direction; $\rho$ and $\rho_G$ are the liquid and bubble densities; $D$, $A$ and $v$ are the bubble diameter, cross sectional area and volume; $c_D$ is the drag coefficient and $\nu$ is the kinematic viscosity. The inertia term on the l.h.s. side of [1] includes the virtual (added) mass $\lambda\rho V$. The coefficient $\lambda$ for a spherical bubble

†It is noted that [1] corresponds to a no-slip condition on the interface. A somewhat difference formulation exists for the case of zero stress at the bubble surface (see Morrison & Stewart 1976). According to Moore (1965), the no-slip formulation applies to ordinary water, which always contains significant amounts of impurity.

can be written as (see Prosperetti & van-Wijngaarden 1976):

$$\lambda = \frac{1}{2}(1 + 2.78\alpha) + 0(\alpha^2) \qquad [3a]$$

or (Ishii & Zuber 1979):

$$\lambda = \frac{1}{2}\frac{1+2\alpha}{1-\alpha} = \frac{1}{2}(1+3\alpha) + 0(\alpha^2) \qquad [3b]$$

where $\alpha$ is the void fraction. In these forms, the interaction of the bubbles is taken into account. When the void fraction $\alpha$ is small ($\alpha \ll 1$), the apparent mass coefficient tends to the value $\lambda = 1/2$ for a single bubble (see also Wallis 1965). For the experimental conditions reported below, the void fractions were very small, particularly behind the shock. Moreover, the variations of $\alpha$ are also very small. Therefore, the virtual mass coefficient is taken as $\lambda = 1/2$ in the following analysis.

The first term on the r.h.s. of [1] represents the pressure forces acting on the bubble. Again this term can be neglected behind the shock. These approximations are discussed below in view of the experimental results.

The third term on the r.h.s. of [1] is the body force (buoyancy) and the last term is the Basset force, which includes the effects of the boundary layer development on the accelerating bubble.

The drag coefficient $c_D$ in the second term of the equation depends on the flow regime, characterized by the Reynolds number, $\mathrm{Re} = wD/\nu$. For relatively low values of Re, the drag coefficient is given by 24/Re, corresponding to Stoke's drag force, which is linear in the relative velocity. This relation holds even for Reynolds numbers high enough for inertia forces to dominate over viscous forces, but only until considerable bubble deformations occur (at $\mathrm{Re} > 400$) (see Peebles & Garber 1953). This case was considered by van-Wijngaarden (1970, 1972). For the experimental conditions of the present work, the Reynolds number range was 2000–12,000; the solution of [1] with $c_D = 24/\mathrm{Re}$ (see Appendix), does not agree, indeed, with the data.

According to Peebles & Garber (1953) and Ishii & Zuber (1979), the drag coefficient in this range of the Reynolds number is nearly constant, $c_D = 2.6$. This value is therefore adopted in the following analysis.

With these assumptions and observing also that $\rho_g \ll \rho$, [1] reduces to:

$$\frac{\mathrm{d}w}{\mathrm{d}t} = -B|w|w - 2g - E\int_0^t \frac{\mathrm{d}w/\mathrm{d}t'}{\sqrt{(t-t')}}\,\mathrm{d}t' \qquad [4]$$

where

$$B \equiv \frac{c_D A}{V}, \qquad E \equiv \frac{3\pi D^2}{V}\frac{(\nu)^{1/2}}{\pi}. \qquad [5]$$

Equation [4] is written now in the following non-dimensional form:

$$\frac{\mathrm{d}W}{\mathrm{d}\tau} = -|W|W - \psi^2 - \phi\int_0^\tau \frac{\mathrm{d}W/\mathrm{d}\tau'}{\sqrt{(\tau-\tau')}}\,\mathrm{d}\tau' \qquad [6]$$

where

$$W \equiv \frac{w}{w_0}, \qquad \tau \equiv \frac{t}{t^*}, \quad \psi^2 \equiv \frac{2g}{Bw_0{}^2}, \quad \phi = \frac{E}{(Bw_0)^{1/2}} \qquad [7]$$

$w_0$ is the initial relative velocity and the characteristic time is defined by:

$$t^* \equiv (Bw_0)^{-1}. \qquad [8]$$

In the following, several approximate solutions of [6] are given for various time domains. Another solution, for small Reynolds numbers were $c_D = 48/\mathrm{Re}$, is given in the Appendix.

For small times (after the shock), the buoyancy forces are small compared to the drag forces, thus $\psi^2$ can be neglected in [6]. The integro-differential equation can then be solved in the following manner: first, the dependent variable $W$ is written in terms of $\mathrm{d}W/\mathrm{d}\tau$. Equation [6] reduces than to an integral equation for the latter which is solved analytically by the method of successive approximations (see Wittaker & Watson 1962). The resulting solution is then integrated once to yield the dimensionless relative velocity $W$. The solution, which satisfies the initial condition $W = 1$ ($w = w_0$) at $\tau = 0$, is given in the form of the series:

$$W = 1 - \tau + \frac{4}{3}\phi\tau^{3/2} + \left(1 - \frac{\pi}{2}\phi^2\right)\tau^2 - \frac{16}{15}\phi\left(2 - \frac{\pi}{2}\phi^2\right)\tau^{5/2} + 0(\tau^3). \qquad [9]$$

This solution can also be rearranged in the following manner:

$$W = 1 - \tau + \tau^2 + \cdots + \frac{4}{3}\phi\tau^{3/2} - \frac{\pi}{2}\phi^2\tau^2 - \frac{16}{15}\phi\left(2 - \frac{\pi}{2}\phi^2\right)\tau^{5/2} + \cdots + 0(\tau^3). \qquad [10]$$

As can easily be seen, the first terms in [10] are also the first terms in the expansion of:

$$W = \frac{1}{1+\tau} \qquad [11]$$

which is the solution of [6] for intermediate times, when the buoyancy term can still be neglected and the Basset force effects tend to vanish. The expansion in series of [11] is valid in the range $\tau \leq 1$ and the first three term of this expansion and also in [10] are within 10 per cent accuracy for $\tau < 0.4$. A comparison of the solutions [10] and [11] is shown in figure 1 for $\phi = 0.044$ which corresponds to the experimental conditions of both runs listed in table 1. The figures also includes the curve given by the first three terms of the series expansion. As can be seen, the effect of the Basset force is very small; the correction, represented by the terms including $\phi$ in [10] is less than 1 per cent of the series expansion. For longer times, the Basset force becomes less significant. The approximate solution[11] is therefore used in section 4 for the comparison with the experimental data.

Finally, [6] is solved for longer times, where the Basset force can be neglected and the buoyancy term is important. The solution is given in two parts; the first:

$$W = \frac{1 - \psi tg\psi\tau}{1 + \frac{1}{\psi}tg\psi\tau}, \qquad 0 \leq \tau \leq \tau_0 = \frac{1}{\psi}\,\mathrm{arc}\,tg\frac{1}{\psi} \qquad [12a]$$

is for the decrease of the relative velocity until it reaches zero value at the time indicated in [12a]. Then the rise of the bubble is given by:

$$W = \psi\frac{\exp[2\psi(\tau - \tau_0)] - 1}{\exp[2\psi(\tau - \tau_0)] + 1} \qquad \tau \geq \tau_0 \qquad [12b]$$

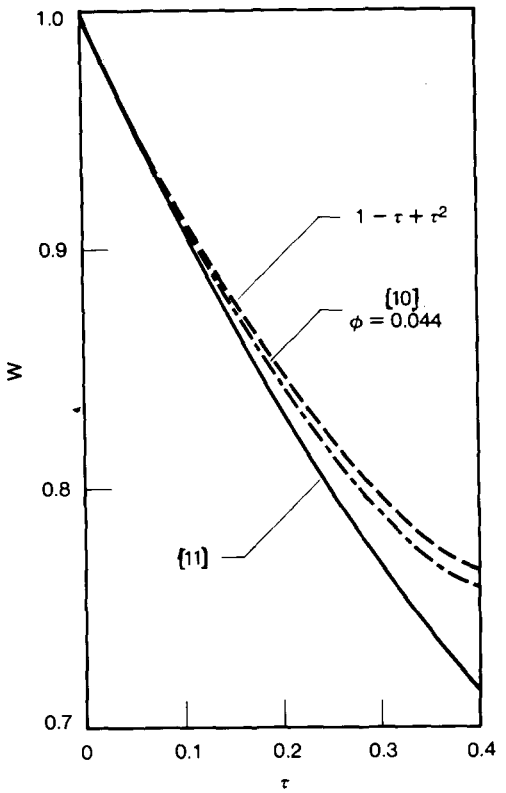


Figure 1. Comparison of approximate solutions for the relative bubble velocity.

Table 1. Measured and calculated parameters for the examples in figures 3–6

| | Run 1<br>Figures 3(a), 4, 6 | Run 2<br>Figures 3(b), 5, 6(b) |
|---|---|---|
| $p_1$—initial pressure, MPa | 0.1 | 0.1 |
| $\rho$—liquid density (water), kg/m$^3$ | 1000 | 1000 |
| $\nu$—liquid kinematic viscosity (water at 300 K), m$^2$/s | $0.8 \times 10^{-6}$ | $0.8 \times 10^{-6}$ |
| $U$—shock velocity, m/s | 97 | 181 |
| $p_2/p_1$—pressure ratio, figure 3 | 2.47 | 2.50 |
| $c_1$—"velocity of sound", m/s | 61.7 | 114 |
| $\alpha_1$—void fraction before the shock, | | |
| isothermal | 0.0270 | 0.0077 |
| adiabatic | 0.0340 | 0.0096 |
| $\alpha_2$—void fraction behind the shock, | | |
| isothermal | 0.0109 | 0.0031 |
| adiabatic | 0.0178 | 0.0050 |
| $u$—liquid velocity behind the shock, m/s | | |
| isothermal | 1.55 | 0.83 |
| adiabatic | 1.57 | 0.84 |
| $w_0$—initial relative bubble velocity (figure 6), m/s | 2.8 | 2.2 |
| $D$—bubble diameter, mm | 3.8 | 5.0 |
| $B$—drag paremeter, [5], m$^{-1}$ | 1030 | 780 |
| $E$—Basset force parameter, [5], s$^{-1/2}$ | 2.39 | 1.82 |
| $\phi$—dimensionless parameter, [7] | 0.0445 | 0.0439 |
| Air flow rate, cm$^3$/s | 4.20 | 2.73 |
| $j_g$—superficial velocity, m/s | 0.0064 | 0.0042 |
| $v_t$—terminal velocity, m/s | 0.225 | 0.585 |
| $\alpha_1$—[21] | 0.0287 | 0.0072 |

and the terminal velocity $W = \psi$ is approached. For small times, again [12a] yields:

$$W = \frac{1 - \psi^2 \tau}{1 + \tau}. \qquad [13]$$

The value of $\psi$ corresponding to the experimental conditions was very small, e.g. $\psi^2 = 0.0052$ for Run 2, with $B = 780\,\mathrm{m}^{-1}$ and $w_0 = 2.2$ m/s (see table 1 and [8]). Therefore, for the time intervals relevant to the experiments, gravity has a negligible effect and [13] reduces to the solution [11]. As mentioned above, the latter is compared to the data in section 4.

The solutions given above are for the relative bubble velocities. In the experiments, only absolute bubble velocities were measured. The liquid velocities needed for comparisons of the experimental and analytical results were estimated from the measured shock conditions (in the following way), based on the derivations of Campbell & Pitcher (1958), van-Wijngaarden (1970, 1972) and Noordzij & van-Wijngaarden (1974). Mass conservation considerations in a coordinate system moving with a shock whose velocity is $U$, which propagates into a liquid at rest, lead to:

$$\rho(1 - \alpha_2)(u + U) = \rho(1 - \alpha_1) U \qquad [14]$$

where $u$ is the liquid velocity behind the shock and the subscripts 1 and 2 refere to the conditions before and after the shock. For small void fractions $\alpha_1$, $\alpha_2 \ll 1$, which is the case considered here, the last relationship reduces to:

$$u = U(\alpha_2 - \alpha_1). \qquad [15]$$

The void fractions could only be roughly estimated from the photographs taken of the bubbly mixture, because of the small void values. Therefore, $\alpha_1$ and $\alpha_2$ were derived by the following method, according, again, to van-Wijngaarden (1070, 1972), Cambell & Pitcher (1958) and Noordzij & van-Wijngaarden (1974). The ratio of void fractions is related to the pressure ratio by:

$$\frac{\alpha_2}{\alpha_1} = \left(\frac{p_2}{p_1}\right)^{1/\gamma} \qquad [16]$$

where $\gamma$ is the ratio of specific heats of the bubble if the process can be regarded as adiabatic and $\gamma = 1$ if the temperature differences are small and isothermal conditions can be assumed.

The shock equations also lead to the following relationship:

$$\frac{U^2}{c_1^2} = \frac{\dfrac{p_2}{p_1} - 1}{1 - \left(\dfrac{p_1}{p_2}\right)^{1/\gamma}} \qquad [17]$$

where the isothermal "velocity of sound" $c_1$ for the bubbly mixture is given by:

$$c_1^2 = \frac{p_1}{\rho \alpha_1 (1 - \alpha_1)}. \qquad [18]$$

The measurable quantities in [14] to [18], are the shock velocity $U$ and the pressures $p_1$ and $p_2$. The void fractions $\alpha_1$, $\alpha_2$ and liquid velocity $u$ can be calculated from these relations. First, the "velocity of sound" $c_1$ is obtained from [17] and introduced into [18] to yield the following

equation for $\alpha_1$:

$$\alpha_1(1-\alpha_1)=\frac{p_1}{\rho U^2}\frac{\frac{p_2}{p_1}-1}{1-\left(\frac{p_1}{p_2}\right)^{1/\gamma}} \qquad [19]$$

and $\alpha_2$ is then found from [15].

The values corresponding to the experiments are given in table 1 and the results are discussed in section 4. It is noted that [19] has two solutions for $\alpha_1$, but only the one representing the small void fraction is relevant.

For low void fractions, $\alpha_1$ can be neglected with respect to 1 in the l.h.s. of [19]. The resulting repression for $\alpha_1$, together with the value of the void fraction behind the shock $\alpha_2$, given by [16], lead to the following expression for the liquid velocity:

$$u=\frac{p_1\left(\frac{p_2}{p_1}-1\right)}{\rho U} \qquad (20)$$

which holds for both isothermal and adiabatic conditions. This result could, indeed, be expected for low void fractions. The results in table 1 were obtained by an exact solution of [19] for isothermal andadiabatic solutions.

## EXPERIMENTAL

The objectives of the experiments were to gather data on transient bubbly mixture flows and to gain information about interphase momentum transfer (by comparison with the analysis). In order to achieve transient motion of air bubbles, these were accelerated in water by the propagation of shock waves. The experiments were performed in a vertical shock tube ($2.5 \times 2.5\ cm^2$, 1.2 m long) as shown in figure 2. High pressure and low pressure sections were separated by a thin diaphragm. A rupture mechanism instantaneously ruptured the diaphragm which initiated the compression/shock waves into the low pressure section containing the two-phase (bubbly) mixture. The volumetric flow of air through the vertical column of water was controlled for obtaining various void values of the mixture. The propagation speed of the wave was monitored by using two pairs of pressure transducers (Piezotrons) which were checked, first, against the calibration and time response by using known pressure pulses. The first pair above the two-phase mixture level provided the propagation speed in air whereas the second pair within the two-phase column provided data on the two-phase propagation speed.

A Schlieren arrangement, with two first surface parabolic mirrors and a laser light source (see figure 2), was used for high speed photography of the shock wave passage through the two-phase column. The framing rates were in the range of $2500 \div 4500$ frames/s, which enabled gathering of enough information for tracking the bubble movement after the shock wave impact. A digitizer was used in tracing the bubble motion with respect to a fixed frame of reference at different instants of time. This data was also used to form bubble velocity profiles.

The pressure signals at two axial locations in the two-phase mixture are shown in figures 3(a,b) for two different experimental runs. From these pressure histories, the transit times for a wave between two locations, at a fixed distance apart, were measured; this yielded direction measure of the average propagation speed of the wave in the bubbly flow. High-speed movies were taken using the optical Schlieren technique. The post-shock bubble movements as captured on the high speed movie frames are shown in figures 4 and 5 for two typical cases. The first frame in rach figure shows a bubble before the shock arrival and the subsequent frames show the bubble motion induced by the shock wave. Note that the bubble is in an upward motion before the short wave impact (see also table 1). Selected movie frames after shock wave

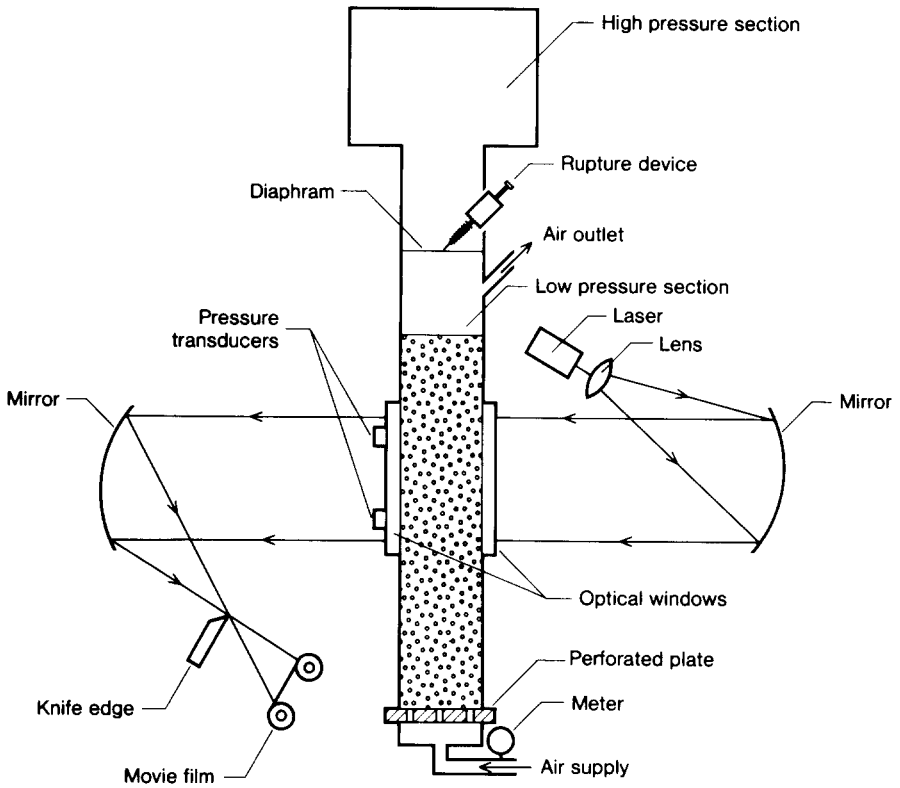


Figure 2. Schematic of the experimental setup.

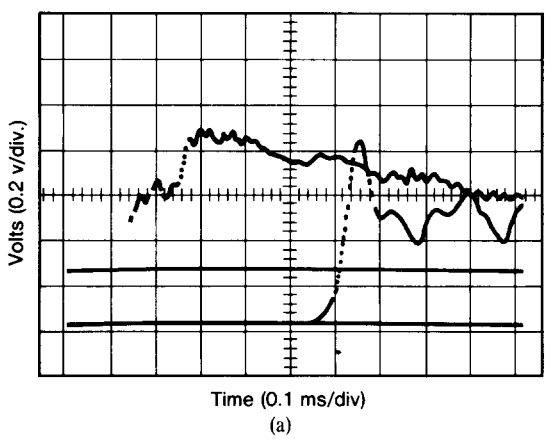


(a)

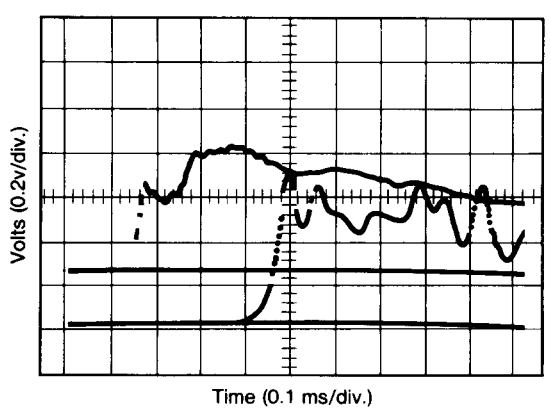


(b)

Figure 3. Pressure histories: (a) Run 1 (see table 1), (b) Run 2 (see table 1).

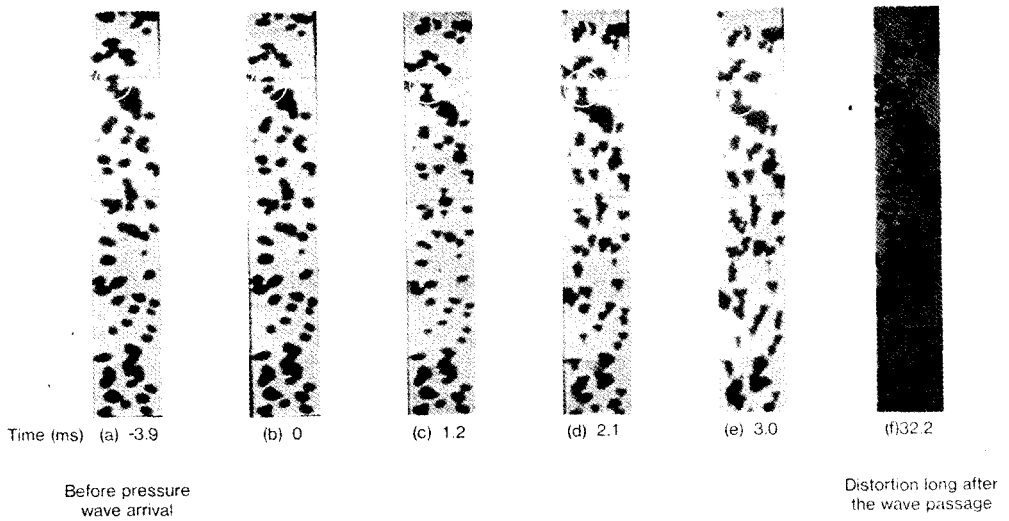


Figure 4. Bubble motion behind the shock (Run 1).

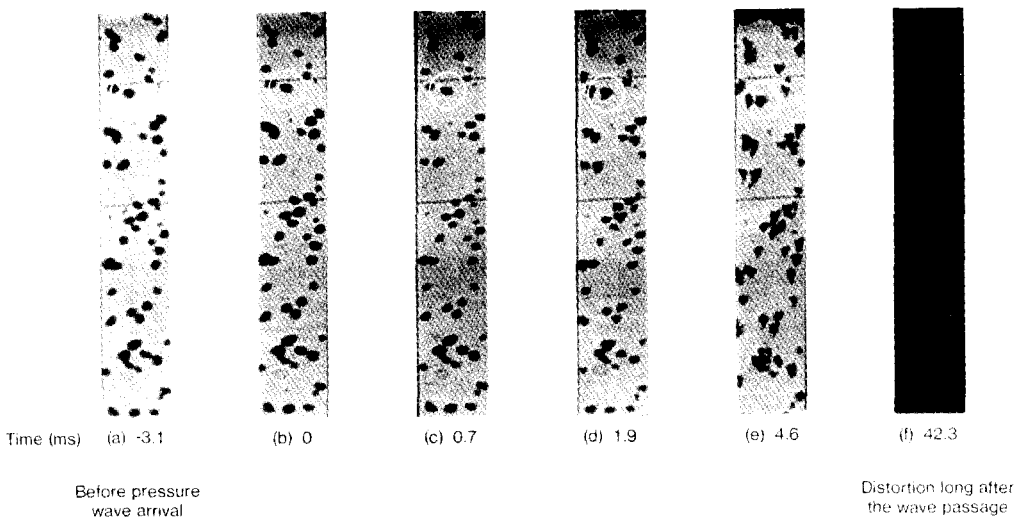


Figure 5. Bubble motion behind the shock (Run 2).

impacts were digitized to obtain bubble trajectories. The velocity histories of two bubbles, measured by this method are shown in figures 6(a, b).

## RESULTS AND DISCUSSION

The behavior of the bubbly mixture flow induced by a shock wave was observed from the high-speed movies (see figures 4 and 5). Prior to the shock impact, the bubbles rose in the column due to buoyancy. The shock, propagating downward, induces a liquid flow behind it in the same direction (this motion cannot be observed in the figures because there is no reference point in this phase). In addition, the shock causes a step acceleration of the bubble in the same direction. This acceleration overcomes the buoyancy force and drives the bubble downwards (see figures 4 and 5), with a speed exceeding that of the liquid. This relative motion is associated with a drag force, which decelerates the bubble. Ideally, the bubble will decelerate to the liquid velocity and then the relative motion will reverse due to buoyancy and a terminal relative velocity will be established. However, as can be seen from figures 4 and 5, the process is quite complex. For example, the impact of the incident shock wave causes deformation of the bubbles; the portion of the bubble facing the shock tends to flatten. The

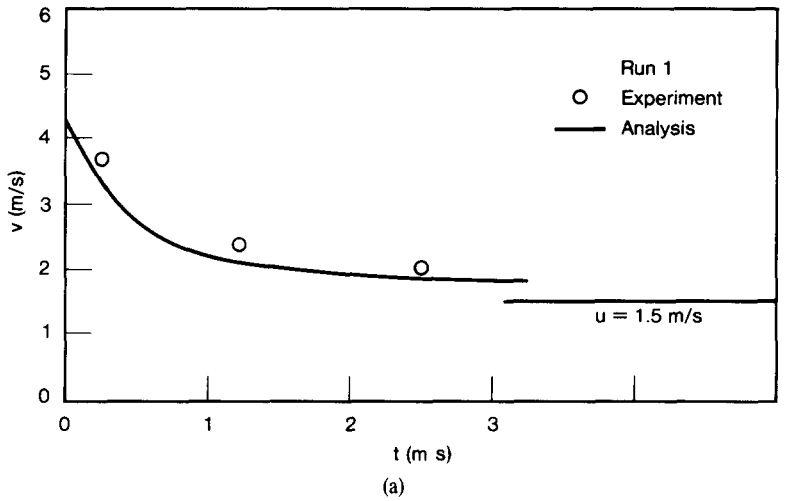


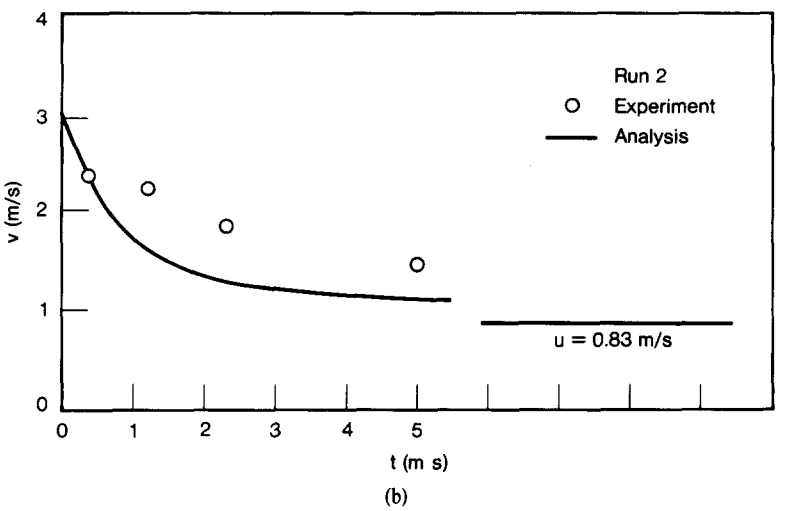


Figure 6. Bubble velocity profiles—experimental and analytical results (a) Run 1 (see table 1), (b) Run 2 (see table 1).

bubble then oscillates and the impact of the reflected waves will cause more distortions (see figures 4 and 5). For example, Hermans (1974) found that a pressure pulse may cause a bubble-surface instability. Gel'fand *et al.* (1975) observed that for a bubble size of 4 mm and 5 per cent void fraction, a pressure difference of 2 MPa causes complete shattering of the bubble. Under these conditions, the velocity of the shock is 300 m/s (Mach 5).

The results for the bubble motions (figures 4 and 5) are for time durations which are smaller than that required for the shock to be reflected from the bottom: $t_r \sim 2L/U$, where $L$ is the shock tube length (1.2 m) and $U$ is the shock speed, which is much larger than the liquid velocity (see table 1). $t_r$ is of the order of 20 ms, while the test durations did not exceed 6 ms (see figure 6).

The results for the two examples reported above are listed in table 1. As can be seen, the void fractions which were calculated by [19] are very small.† Therefore, a direct measurement

†This also justifies the assumptions on the behavior of the apparent mass coefficient, $\lambda = 1/2$.

of the $\alpha$ and $\alpha_2$ from the photographs in figures 4 and 5 is quite inaccurate. However, values of the void fractions obtained by counting the bubbles and computing their volumes were found to be of the same order of magnitude as those in table 1. The void fraction can also be estimated by the following relationship (see Wallis 1969, Wilson *et al.* 1962):

$$\alpha_1 = j_g/v_t \qquad [21]$$

where $j_g$ is the superficial gas velocity and $v_t$ is the terminal velocity before the shock. The former was calculated from the measured volumetric air flow rate and the latter from the high-speed movies. These values are also listed in table 1. The agreement between the values of $\alpha_1$ calculated by [21] and by the procedure outlined in section 2 for isothermal conditions is very good—within 7 per cent. The adiabatic calculations lead to higher void fraction values.

It is noted that the relaxation time of the thermal processes in the gas phase is $\rho_G C_G D^2/4k_G$ where $k_G$ is the thermal conductivity of the gas (see Noordzij & van-Wijngaarden 1974). This yields a value of 300 ms, which is much larger than the shock durations of 0.2 ms (figure 3) and even the whole experimental times of 6 ms (figure 6). On the other hand, the mixture temperature difference across the shock is given by (see Campbell & Pitcher 1958):

$$\Delta T = \frac{(p_2/p_1)^2 - 1}{2p_2/p_1} \frac{\mu_1 R T_1}{C} \qquad [22]$$

where $\mu_1$ is the mass fraction and $T_1$ the temperature before the shock, $R$ is the gas constant and $C$ the specific heat of the liquit. The temperature difference for the experimental conditions (see table 1) is of the order of 0.001 K. Furthermore, for small void fractions, the liquid velocity behind the shock $u$, given by the approximation [20] is the same for both isothermal and adiabatic conditions. The more accurate values, calculated by [15], [16] and [19] are, indeed, very close for both cases as can be seen from table 1. These considerations show that while for the low-void mixture isothermal relations can be applied (because $\gamma = c_p/c_v \approx 1$), compressibility strongly affects the behavior of the gas phase.

The experimental results for the bubble bubble velocity profiles are plotted in figures 6(a) and 6(b). The curves were extrapolated in order to obtain the initial velocities $w_0$ (at $t = 0$) immediately after the shock. The solution [11] of the relative velocity history was converted to dimensional values for the absolute bubble velocity using [2], [7] and [8], which the values of the parameters are listed in table 1. As can be seen, the agreement between the analytical and experimental results is quite good. This indicates that a simplified analysis, based on a constant drag coefficient $c_D = 2.6$, can be used at least as a first approximation, to characterize the transient bubble motions in the relevant range of Reynolds number 2000–12,000, the former value corresponds to the relative velocities at the termination of the experiments and the latter to the initial velocities (see figure 6 and table 1).

A more detailed analysis will be required in order to interpret more sophisticated experiments and additional complex phenomena. Moreover, the information on the bubble behavior inside the shock is still unavailable. van-Wijngaarden *et al.* (1970, 1972, 1974, 1976) studied the shock behavior and void fractions but these methods have not been extended yet to describe the bubble motions. For example, the bubble velocity at the back of the shock cannot be calculated by any existing theory.

*Acknowledgements*—The authors wish to thank Dr. R. B. Duffey for his helpful comments and suggestions, which have been incorporated into this manuscript.

## REFERENCES

BRODKEY, R. S. 1967 *The Phenomena of Fluid Motions*, p. 621. Addison-Wesley, Reading, Mass.

CAMPBELL, I. J. & PITCHER, A. S. 1958 Shock waves in a liquid containing gas bubbles. *Proc. R. Soc.* **A243**, 534–545.

CRESPO, A. A. 1969 Sound waves in liquid containing bubbles. *Phys. Fluid* **12**, 2274–2282.

GEL'FAND, B. E., GUBIN, S. A., KOGARO, S. M., SIMAKOV, S. M. & TIMOFEEV, E. I. 1975 Disintegration of air bubbles in a liquid by shock waves. *Sov. Phys. Dokl.* **20**, 95–98.

HERMANS, W. A. H. J. 1974 On the instability of a translating gas bubble under influence of a pressure step. Thesis, Endhoven, N74-29643 NTIS.

ISHII, M. & ZUBER, N. 1979 Drag coefficient and relative velocity in bubbly droplet and particulate flows. *AICHE J.* **25**, 843–855.

KARANFILIAN, S. K. & KOTAS, T. J. 1978 Drag on a sphere in unsteady motion in a liquid at rest. *J. Fluid. Mech.* **87**, 85–96.

LANDAU, L. D. & LIFSHITZ, E. M. 1959 *Fluid Mechanics*, p. 97. Pergamon Press, Oxford.

LUGT, H. J. & HAUSSLING, H. J. 1978 The acceleration of thin cylindrical bodies in a viscous fluid. *J. Appl. Mech.* **45**, 1–6.

MOORE, D. W. 1965 The velocity of rise of distorted gas bubbles in a liquid of small viscosity. *J. Fluid Mech.* **23**, 749–766.

MORRISON, F. A. JR. & STEWARD, M. B. 1976 Small bubble motion in an accelerating liquid. *J. Appl. Mech.* **43**, 399–403.

NOORDZIJ, L. 1973 Shock waves in bubble–liquid mixtures. *Proc. IUTAM Symp. Non-Steady Flow of Water at High Speeds* (Edited by L. I. SEDOV and G. YU-STEPANOV) p. 369. Nauka, Moscow.

Noordzij, L. & VAN-WIJNGAARDEN, L. 1974 Relaxation effects, caused by relative motion, on shock waves in gas–bubble/liquid mixtures. *J. Fluid Mech.* **66**, 115–143.

NYER, R. L. & SCHROCK, V. E. 1967 Propagation of shock waves through two-phase two component media. *Trans. Ans.* **10**, 660.

PEEBLES, F. N. & GARBER, H. J. 1953 Studies on the motion of gas bubbles in liquids. *Chem. Engng Prog.* **49**, 88–97.

PROSPERETTI, A. & VAN-WIJNGAARDEN, L. 1976 On the characteristics of the equations of motion for a bubbly flow and the related problem of critical flow. *J. Engng Math.* **10**, 153–162.

TYLER, A. L. & SALT, D. L. 1978 Periodic discontinuities in the acceleration of spheres in free flight. *J. Fluids Engng* **200**, 17–21.

WALLIS, G. B. 1969 *One-Dimensional Two-Phase Flow*. McGraw-Hill, New York.

WHITTAKER, E. T. & WATSON, G. N. 1962 *A Course of Modern Analysis*, p. 221. Cambridge University Press.

WIJNGAARDEN, L. VAN- 1968 On the equations of motion for mixtures of liquid and gas bubbles. *J. Fluid Mech.* **33**, 465–474.

WIJNGAARDEN, L. VAN- 1970 On the structure of shock waves in liquid–bubble mixture. *Appl. Sci. Res.* **22**, 366–381.

WIJNGAARDEN, L. VAN- 1972 Propagation of shock waves in bubble–liquid mixtures. In *Progress in Heat and Mass Transfer*, Vol. 6 (Edited by G. HETSRONI, S. SIDEMAN and J. P. HARTNETT), pp. 637–649. Pergamon Press, New York.

WILSON, I. F., GRENDA, R. J. & PATTERSON, J. F. 1962 The velocity of rising steam in a bubble two-phase mixture. *Trans. Ans.* **5**, 151–152.

## APPENDIX

The equation of motion of the bubble [1] was written in a generalized form; the drag force includes the drag coefficient $c_D$. The equation is solved here for low Reynolds numbers, where $c_D = 24/\mathrm{Re}$. Introducing this correlation into [1], the following form is obtained (with the same

assumptions of section 2):

$$\frac{dw}{dt} = bw - 2g - E\int_0^t \frac{dw/dt'}{\sqrt{(t-t')}}\,dt' \qquad [A1]$$

where $E$ is defined in [5] and

$$b \equiv \frac{3\pi\nu D}{\lambda V} = \frac{36\nu}{D^2}. \qquad [A2]$$

Equation [1] is written in the following non-dimensional form:

$$\frac{dW}{dT} = -W - \Psi^2 - \Phi^2\int_0^T \frac{dW/dT'}{\sqrt{(T-T')}}\,dT' \qquad [A3]$$

where

$$W \equiv \frac{w}{w_0}, \qquad T \equiv bt, \qquad \Psi^2 \equiv \frac{2g}{w_0 b}, \qquad \Phi \equiv \frac{E}{b^{1/2}} \qquad [A4]$$

and $w_0$ is the initial velocity. It is noted that the characteristic time is different than that in section 2. For small times, the buoyancy term $\Psi^2$ can be neglected. The resulting integro-differential equation [A3] is then solved in a manner similar to that used in section 2. The dependent variable $W$ is written in terms of $dW/dT$; the integral equation, resulting from [A3] is solved for the latter by the method of successive approximations and then the solution is integrated once to yield $W$. This leads to the following series form:

$$\begin{aligned} W &= 1 - T + \frac{4}{3}\Phi T^{3/2} + \left(\frac{1}{2} - \frac{1}{2}\pi\Phi^2\right)T^2 - \frac{16}{15}\Phi\left(1 - \frac{\pi}{2}\Phi^2\right)T^{5/2} + \cdots \\ &= 1 - T + \frac{1}{2}T^2 + \cdots + \frac{4}{3} - \frac{1}{2}\pi\Phi^2 T^2 - \frac{16}{15}\Phi\left(1 - \frac{\pi}{2}\Phi^2\right)T^{5/2} \ldots \end{aligned} \qquad [A5]$$

where the first terms represent the expansion of $W = e^{-T}$, which is the solution without the Basset force.

For the experiments reported in this work, the values of $b$ are 1.99 and 1.55 $s^{-1}$ (see [A2] and table 1 for Runs 1 and 2) and $\Phi = 1.70$ for both examples ([A4] and table 1). The durations of the experiments were about 5 ms (figure 6); this gives a range of $6 \times 10^{-3}$ for the dimensionless time $T$ (see [A4]). The solution [A5] yields, then,

$$W = 1 - 6 \times 10^{-3} + 1.1 \times 10^{-3}. \qquad [A6]$$

The deviation from the initial velocity ($W = 1$) is very small and cannot represent the data in figure 6, for which the Reynolds numbers are large. The result [A6] also shows that for lower Reynolds numbers, the Basset force is important—it corresponds to about 22 per cent of the velocity changes.